Supplementary information for:

Distinct intercalation and conduction behaviours within an isostructural series $Ba_5R_2Al_2SnO_{13}$

Alex J. Brown[1], Oliver J. Wagstaff[2], Ivana Radosavljevic Evans [2], John S. O. Evans[2], Richard A. Mole[3], Jeremy Wykes[4], Maxim Avdeev[1,3] and Chris D. Ling[1,]*

1. School of Chemistry, The University of Sydney, Sydney NSW 2006, Australia
2. Department of Chemistry, Durham University, Science Site, South Road, Durham DH1 3LE, U.K.
3. Australian Centre for Neutron Scattering, Australian Nuclear Science and Technology Organisation, Menai 2234, Australia
4. Australian Synchrotron, Australian Nuclear Science and Technology Organisation, 800 Blackburn Road, Clayton 3168, Australia

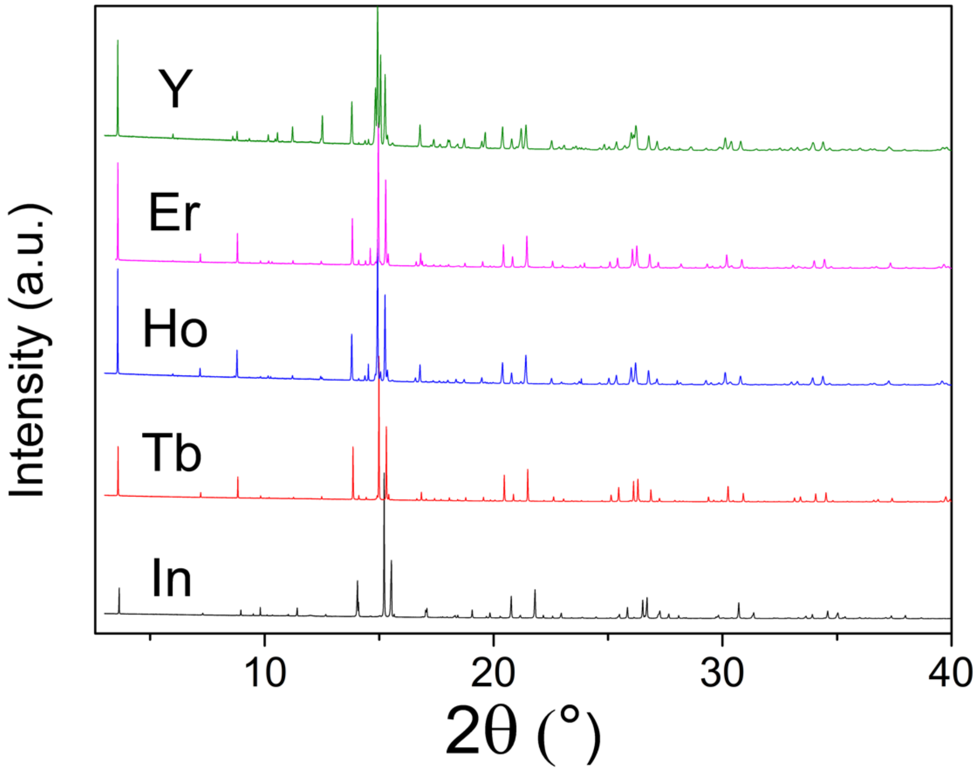

Figure S1 S-XRD data of $Ba_5R_2Al_2SnO_{13}$ (R = In, Tb, Ho, Er, Y) collected at the Australian Synchrotron PD beamline with patterns offset on the y-axis for clarity.

Table S1: refined unit cell parameters for the $Ba_5R_2Al_2SnO_{13}$ (R = In, Tb, Ho, Er, Y) series

Compound	**a (Å)**	**c (Å)**	**Vol (Å^3)**	***R*$^{3+}$ ionic radius (Å)**	**Crystal Density (g/cm^3)**
$Ba_5In_2Al_2SnO_{13}$	5.84716(4)	24.3258(2)	720.271(2)	0.8	5.862(1)
$Ba_5Tb_2Al_2SnO_{13}$	5.9375(6)	24.6604(5)	752.913(4)	0.882 (Tb^{4+})	6.110(1)
$Ba_5Ho_2Al_2SnO_{13}$	5.9595(2)	24.7434(5)	761.051(2)	0.901	6.102(2)
$Ba_5Er_2Al_2SnO_{13}$	5.94611(6)	24.6968(3)	756.221(2)	0.89	6.153(1)
$Ba_5Y_2Al_2SnO_{13}$	5.9586(6)	24.7372(4)	760.638(3)	0.9	6.046(3)

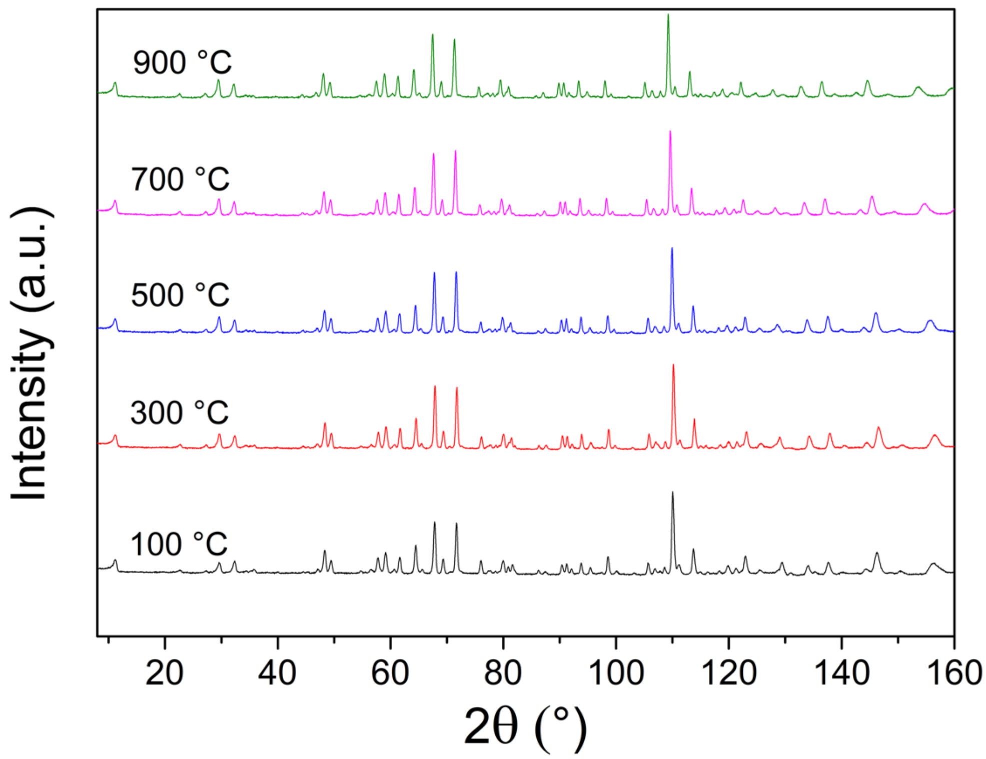

Figure S2 Variable temperature NPD data (λ = 2.4395 Å) of $Ba_5Er_2Al_2SnO_{13}$.

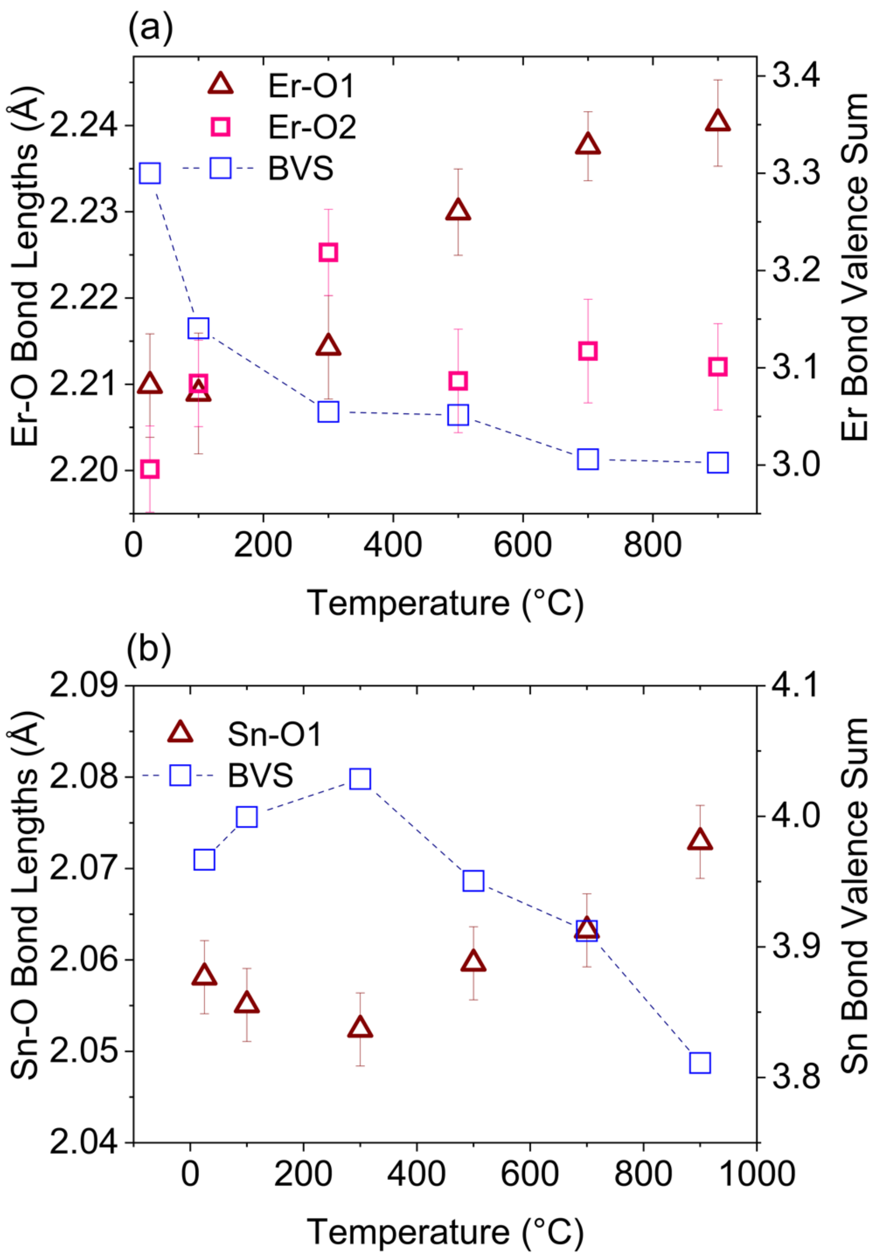

Figure S3 Refined bond lengths and calculated BVS for (a) Er-O and (b) Sn-O in $Ba_5Er_2Al_2SnO_{13}$ from NPD data.

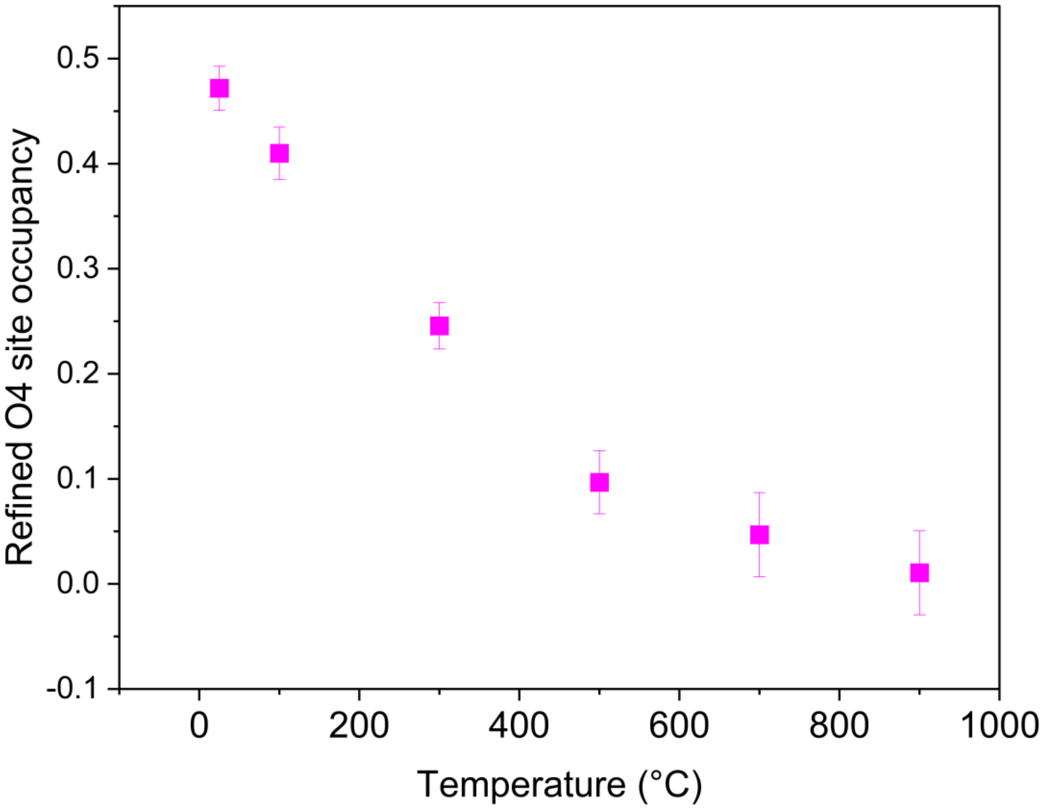

Figure S4 $Ba_5Er_2Al_2SnO_{13}$ refined O(H) occupancy at the O4 (0, 0, 1/4) site. Occupancy falls from ~0.5 at RT to ~0 at 900 °C.

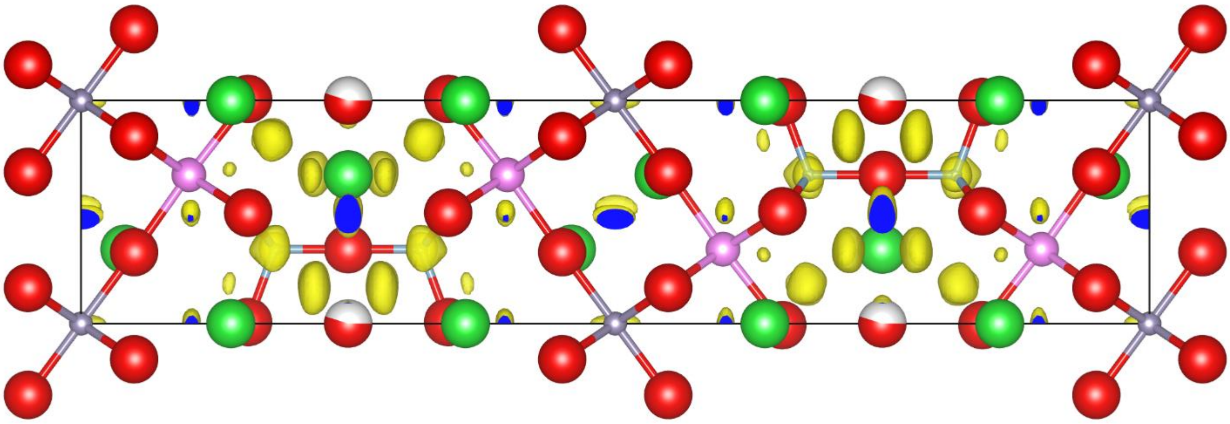

Figure S5 Negative nuclear Fourier difference peaks (yellow) for $Ba_5Er_2Al_2SnO_{13}$ from refinement against RT NPD data. Er atoms are pink, Sn purple, Al light blue, Ba light green, O red. The largest nuclear density differences surround the O3 and O4 atoms.

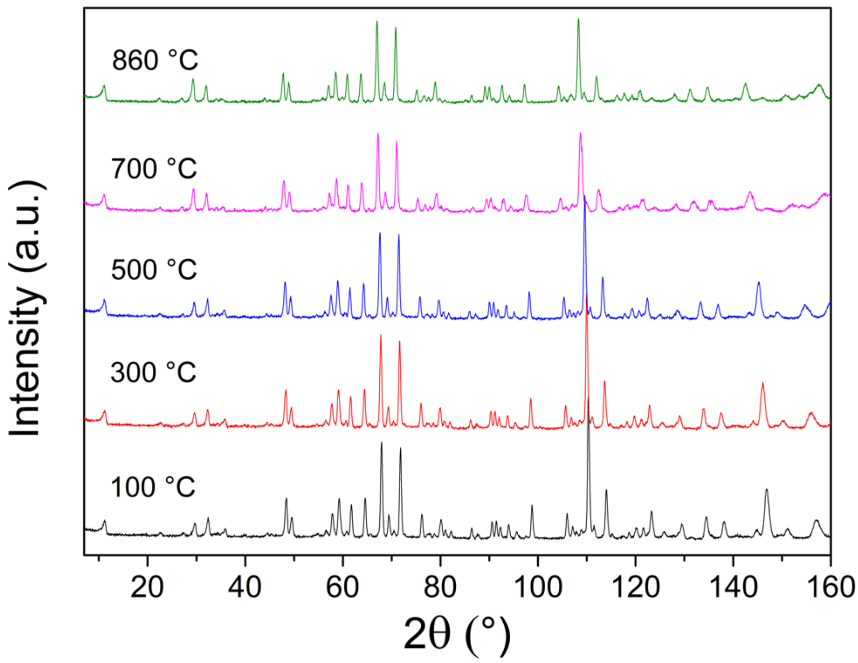

Figure S6 Variable temperature NPD data (λ = 2.4395 Å) from $Ba_5Tb_2Al_2SnO_{13}$.

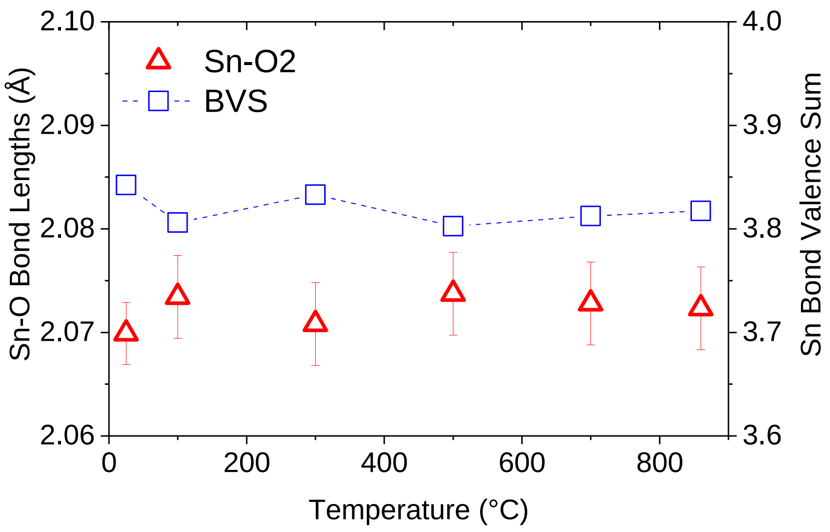

Figure S7 Refined Sn-O bond lengths and bond valence sums for $Ba_5Tb_2Al_2SnO_{13}$ from NPD data. Error bars are smaller than symbols for BVS.

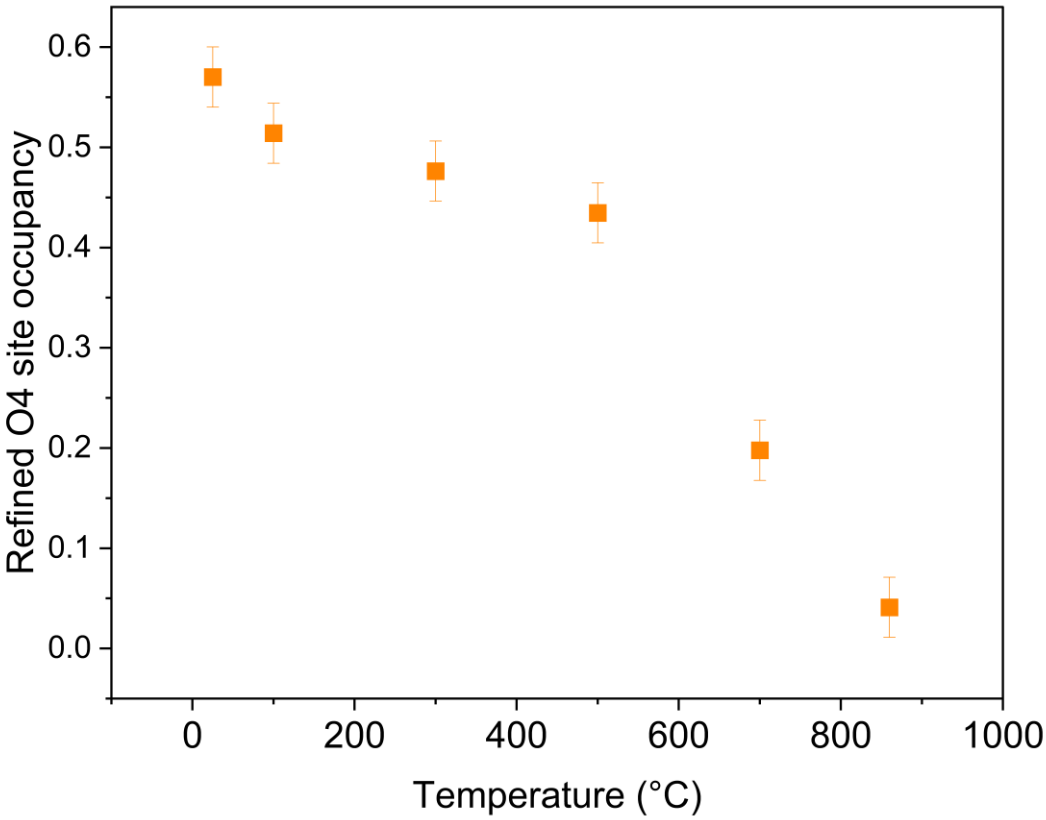

Figure S8 $Ba_5Tb_2Al_2SnO_{13}$ O4 site occupancy from refinement against NPD data.

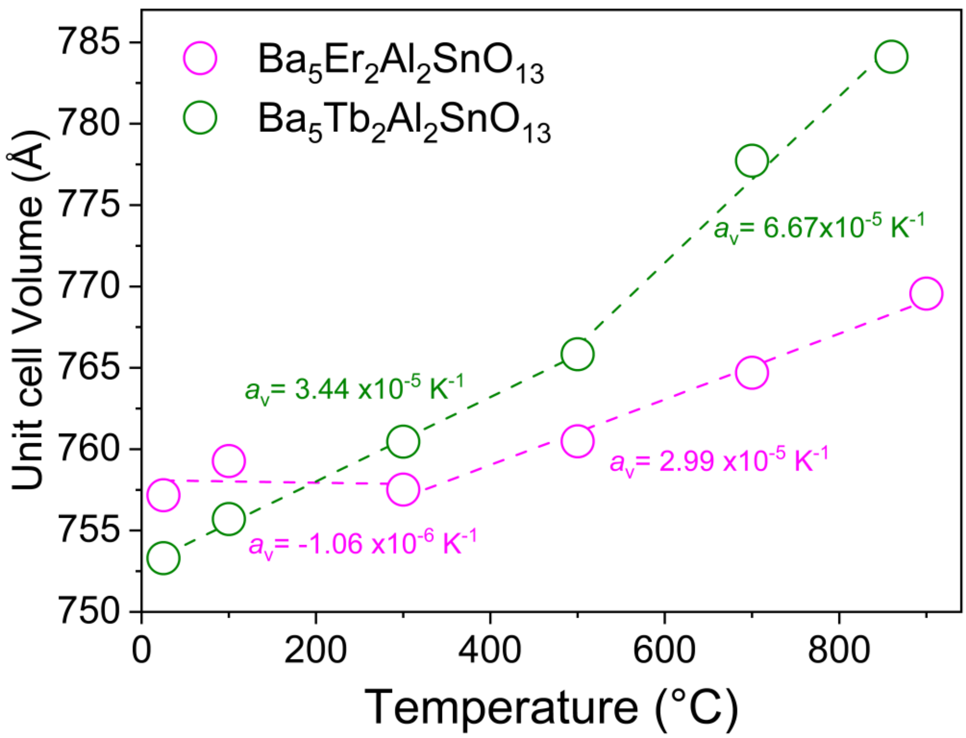

Figure S9 Refined unit cell volumes for $Ba_5Er_2Al_2SnO_{13}$ and $Ba_5Tb_2Al_2SnO_{13}$ from variable temperature NPD. Dashed lines are guides to the eye. Thermal expansion coefficients a_v for the RT-300 °C unit cell volumes and 300-900 °C unit cell volumes are shown for both phases. Error bars smaller than symbols.

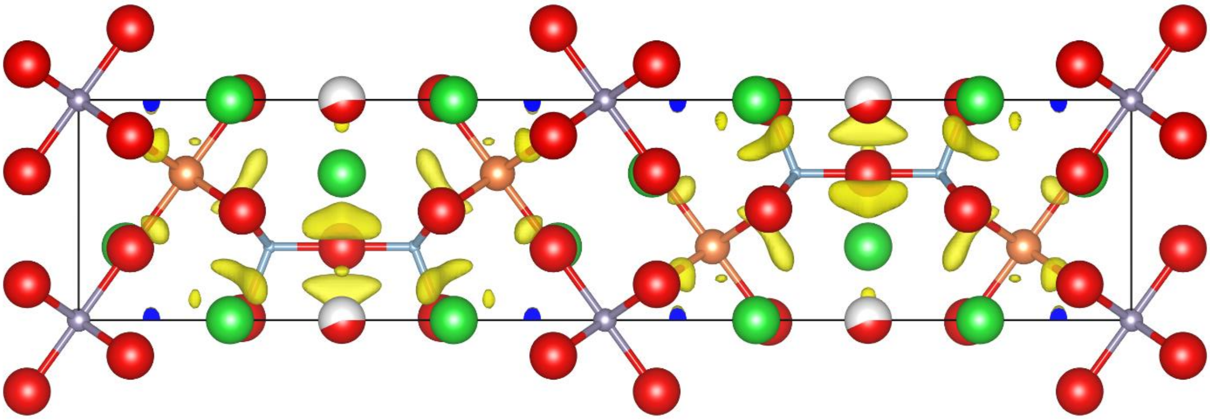

Figure S10 Negative nuclear Fourier difference peaks (yellow) for $Ba_5Tb_2Al_2SnO_{13}$ for refinement against RT NPD data. Tb atoms are orange, Sn purple, Al light blue, Ba light green, O red. As for $Ba_5Er_2Al_2SnO_{13}$ the largest nuclear density differences surround the O3 and O4 atoms.

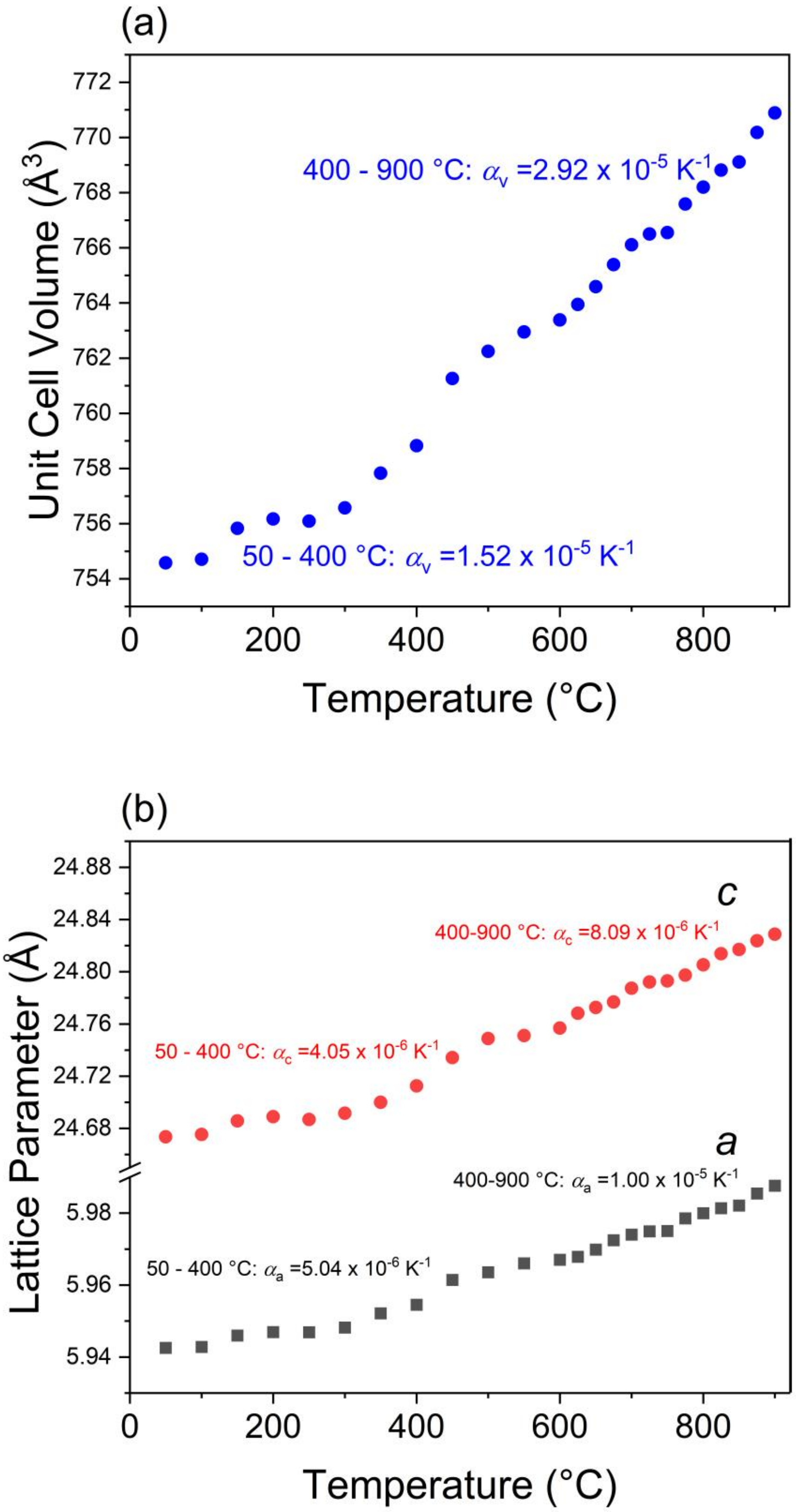

Figure S11 Refined lattice parameters and unit cell volumes determined from variable temperature XRD data of $Ba_5Tb_2Al_2SnO_{13}$ from RT to 900 °C. With thermal expansion coefficients shown for the ranges 50-400 °C and 400-900 °C. Error bars smaller than symbols.

Table S2: Example EDS spectra readouts of the metals for $Ba_5Tb_2Al_2SnO_{13}$ which gives a composition of $Ba_{4.95}Tb_{1.95}Al_{2.07}Sn_{1.02}O_{13.4}$ (assuming mixed Tb^{3+}/Tb^{4+})

Element	*Average At %*
Al	20.7 ± 0.8
Sn	10.2 ± 0.4
Ba	49.6 ± 0.1
Tb	19.5 ± 0.4
Total	100.00

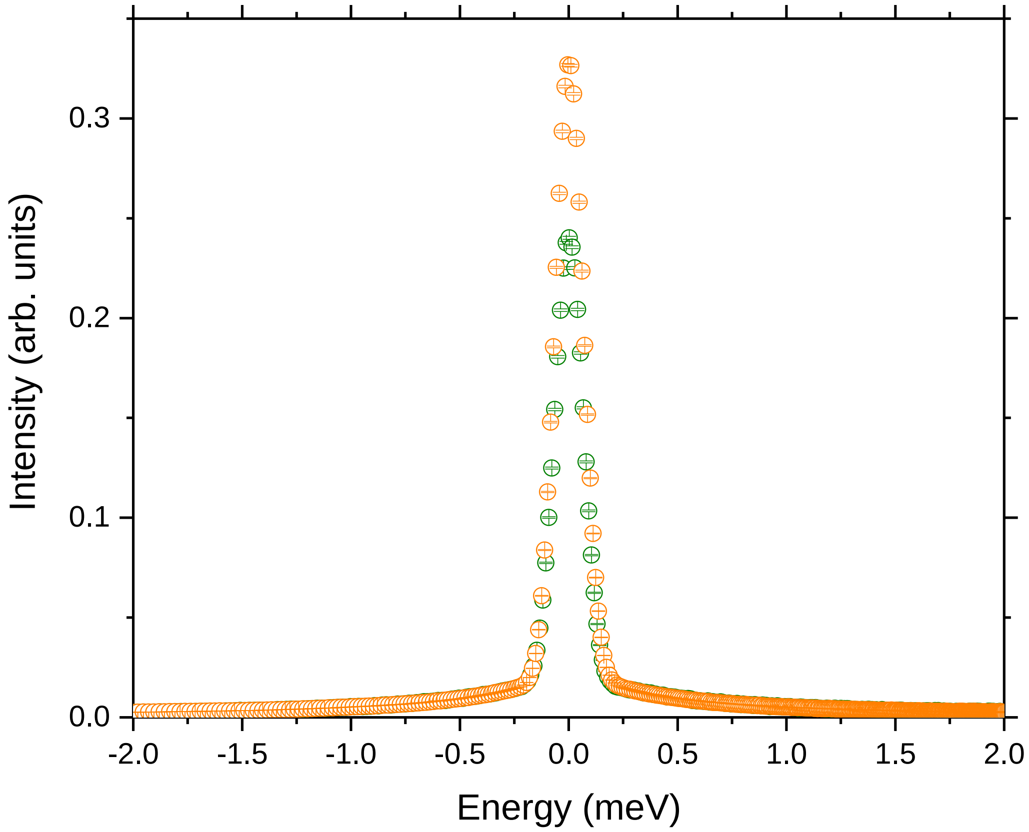

Figure S12: Temperature dependence of the Q-integrated data S(ω) of $Ba_5Er_2Al_2SnO_{13}$. Green markers are 4.69 Å 300 K after dehydration. Orange markers are 4.69 Å 300 K before dehydration.

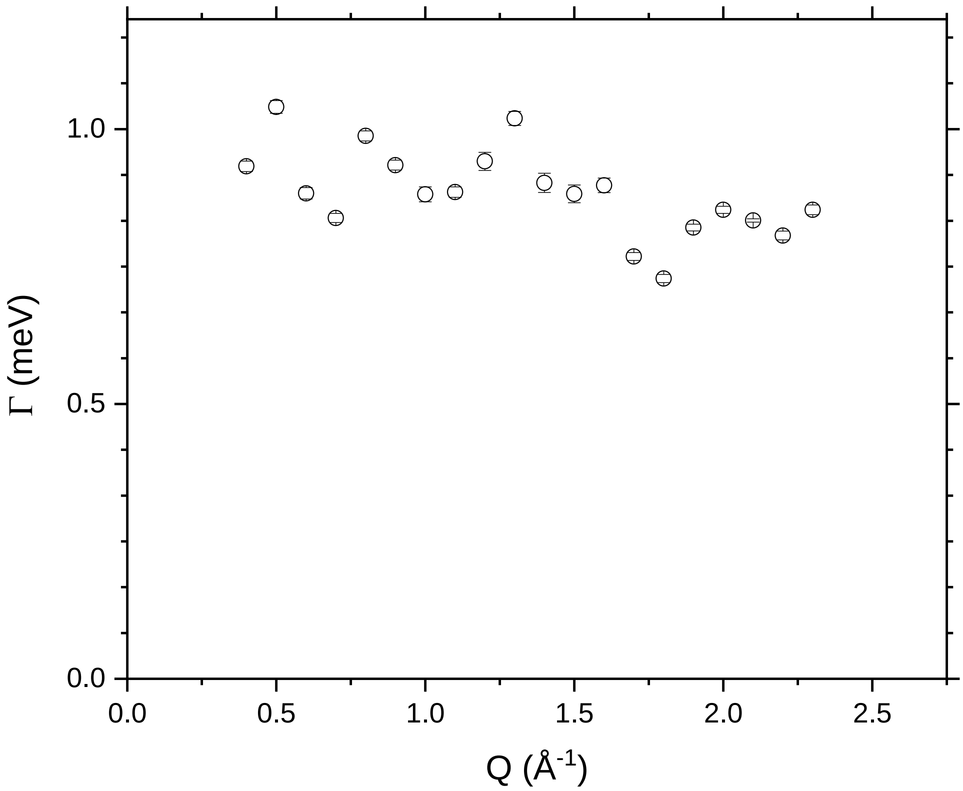

Figure S13: Extracted HWHM against Q of $Ba_5Er_2Al_2SnO_{13}$ for the single Lorentzian components of the fit at 300 K

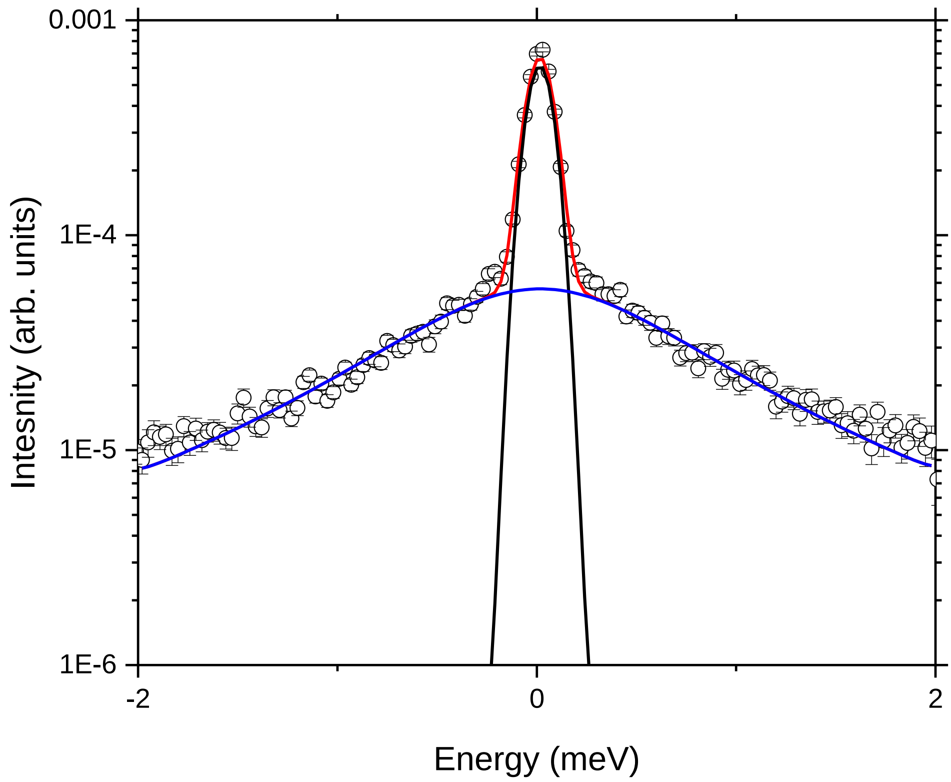

Figure S14: Quasielastic neutron scattering at Q = 1 Å^{-1} for $Ba_5Er_2Al_2SnO_{13}$ measured at 300 K with 4.69 Å neutrons. The blue line is the Lorentzian component convoluted with the instrument resolution function. The black line is a delta peak convoluted with the instrument resolution function. The red line is the total fit.

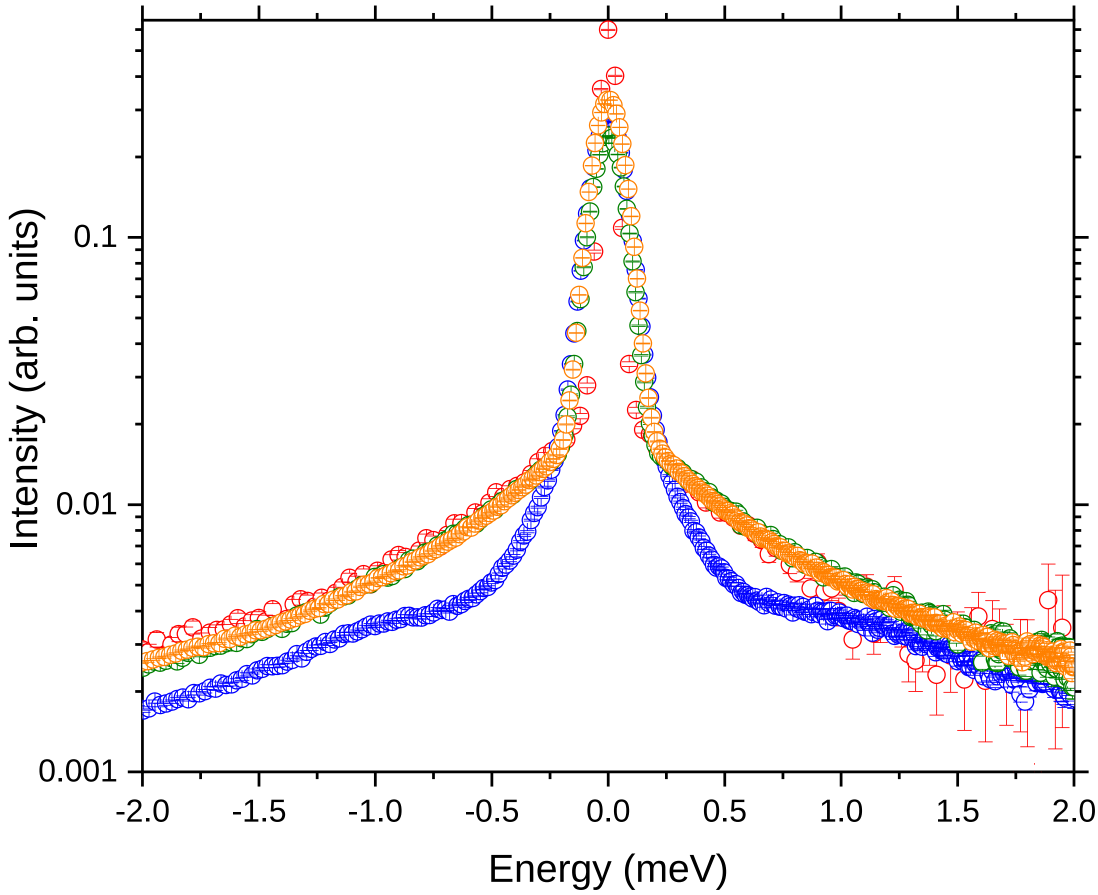

Figure S15: Temperature dependence of the Q integrated data S(ω) for $Ba_5Er_2Al_2SnO_{13}$. Blue markers are 4.69 Å at 100 K, green are 4.69 Å at 300 K, both after dehydration. Orange markers are 4.69 Å at 300 K, red are 5.98 at Å 300 K, both before dehydration.

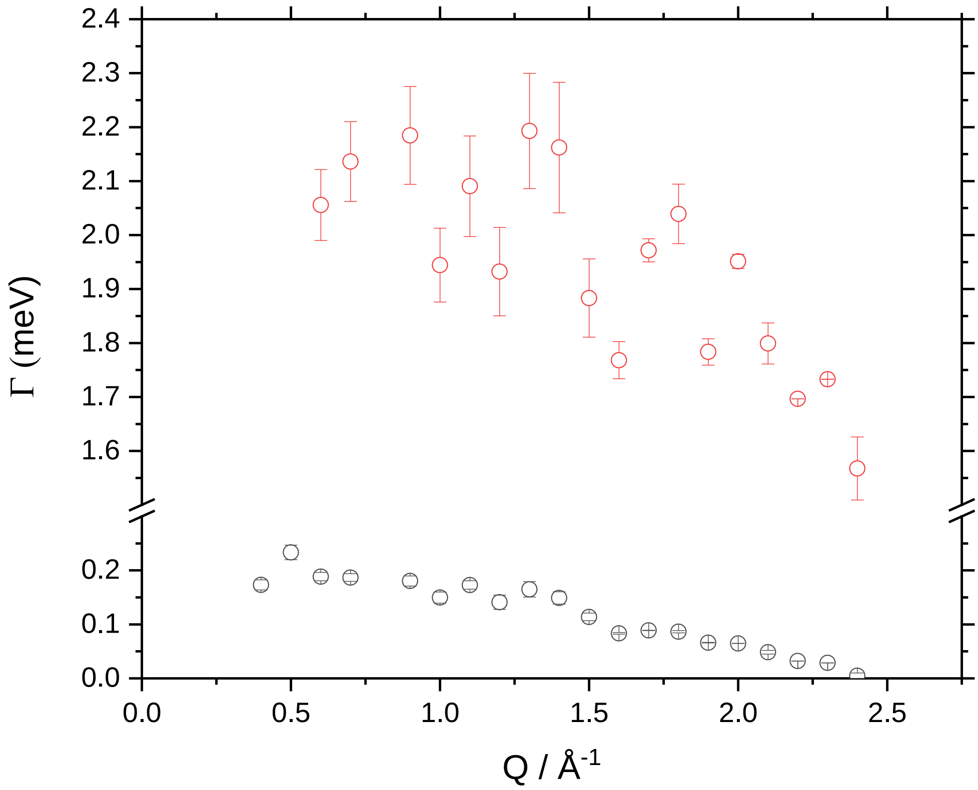

Figure S16: HWHM vs. Q of $Ba_5Er_2Al_2SnO_{13}$ for the two Lorentzian components of the fit to 100 K data.

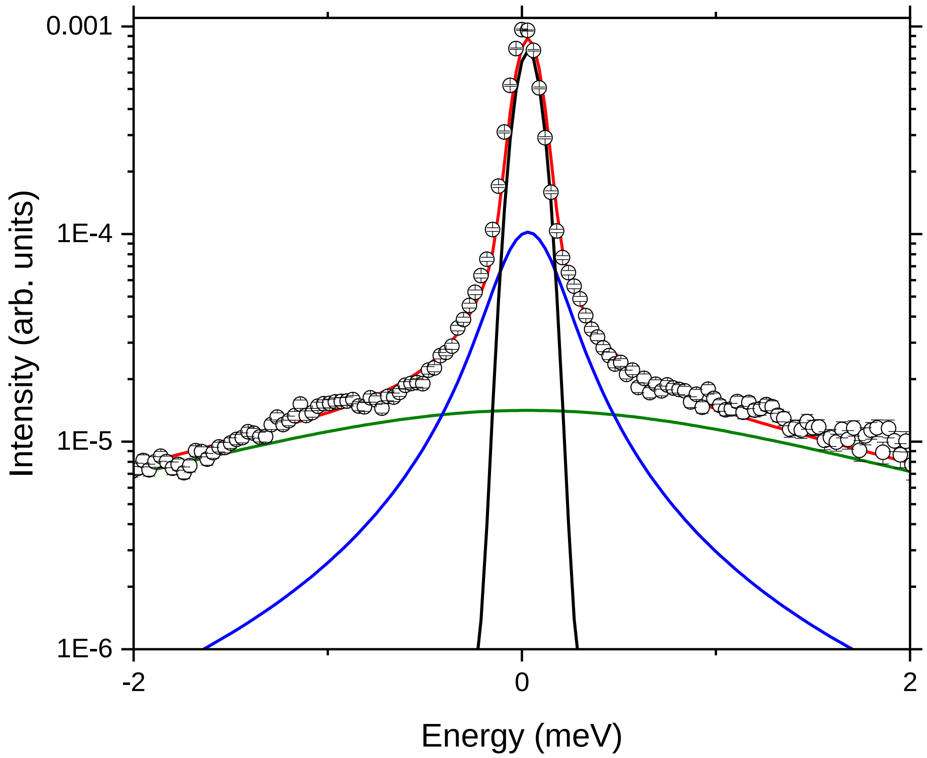

Figure S17: Quasielastic neutron scattering at Q = 1 Å^{-1} for $Ba_5Er_2Al_2SnO_{13}$ measured at 100 K with 4.69 Å neutrons. The blue and green lines are Lorentzian components convoluted with the instrument resolution function. The black line is a delta peak convoluted with the instrument resolution function. The red line is the total fit.

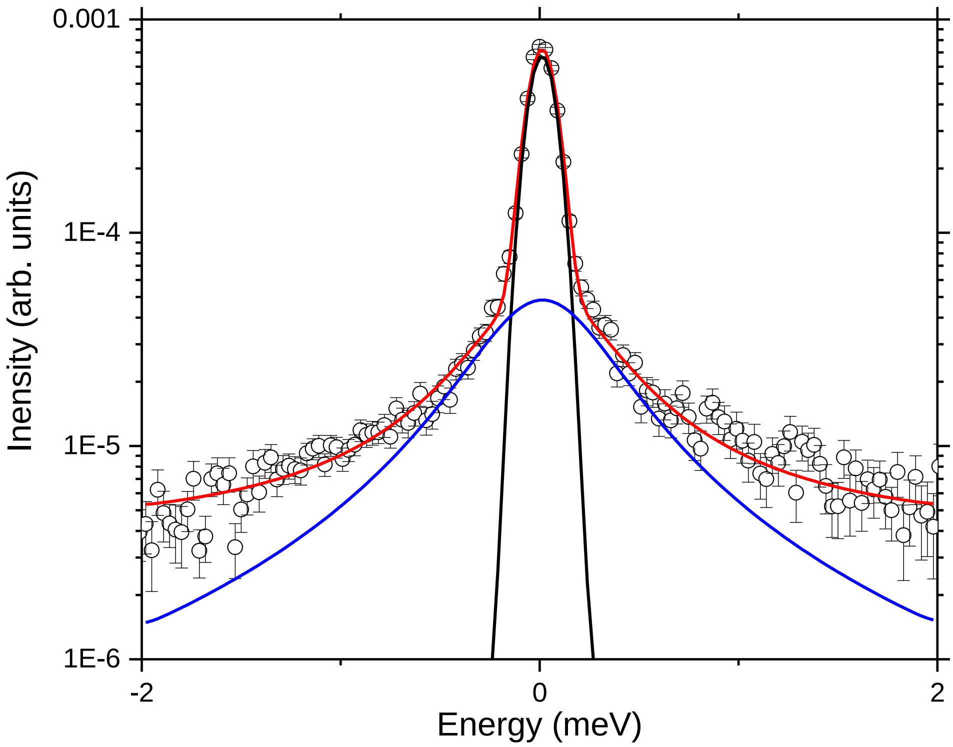

Figure S18: Black data points are quasielastic neutron scattering at Q = 1 Å^{-1} of $Ba_5Tb_2Al_2SnO_{13}$ measured at 300 K with 4.69 Å neutrons. The blue line is the Lorentzian component convoluted with the instrument resolution function. The black line is a delta peak convoluted with the instrument resolution function. The red line is the total fit.

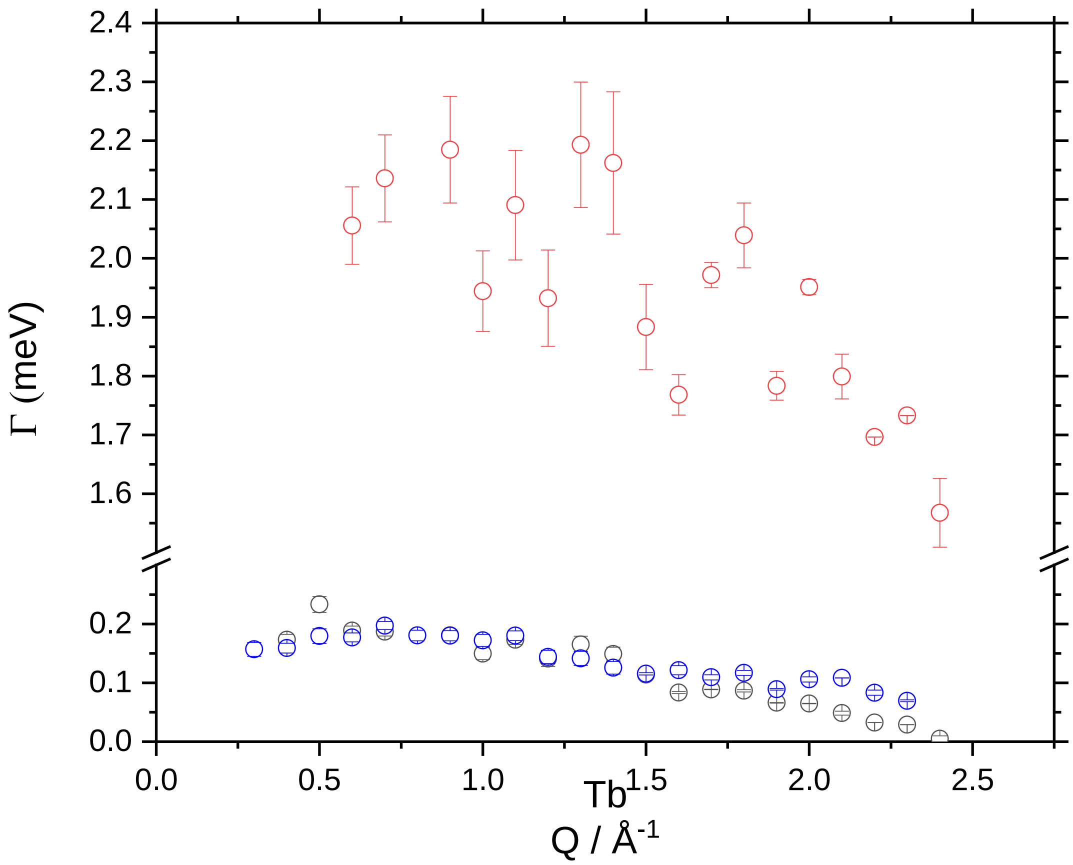

Figure S19: Black and red data points are the HWHM vs. Q for the two Lorentzian components of the fit at 100 K for $Ba_5Er_2Al_2SnO_{13}$. Blue data points are the HWHM vs. Q for the single Lorentzian component of the fit at 300 K for $Ba_5Tb_2Al_2SnO_{13}$.

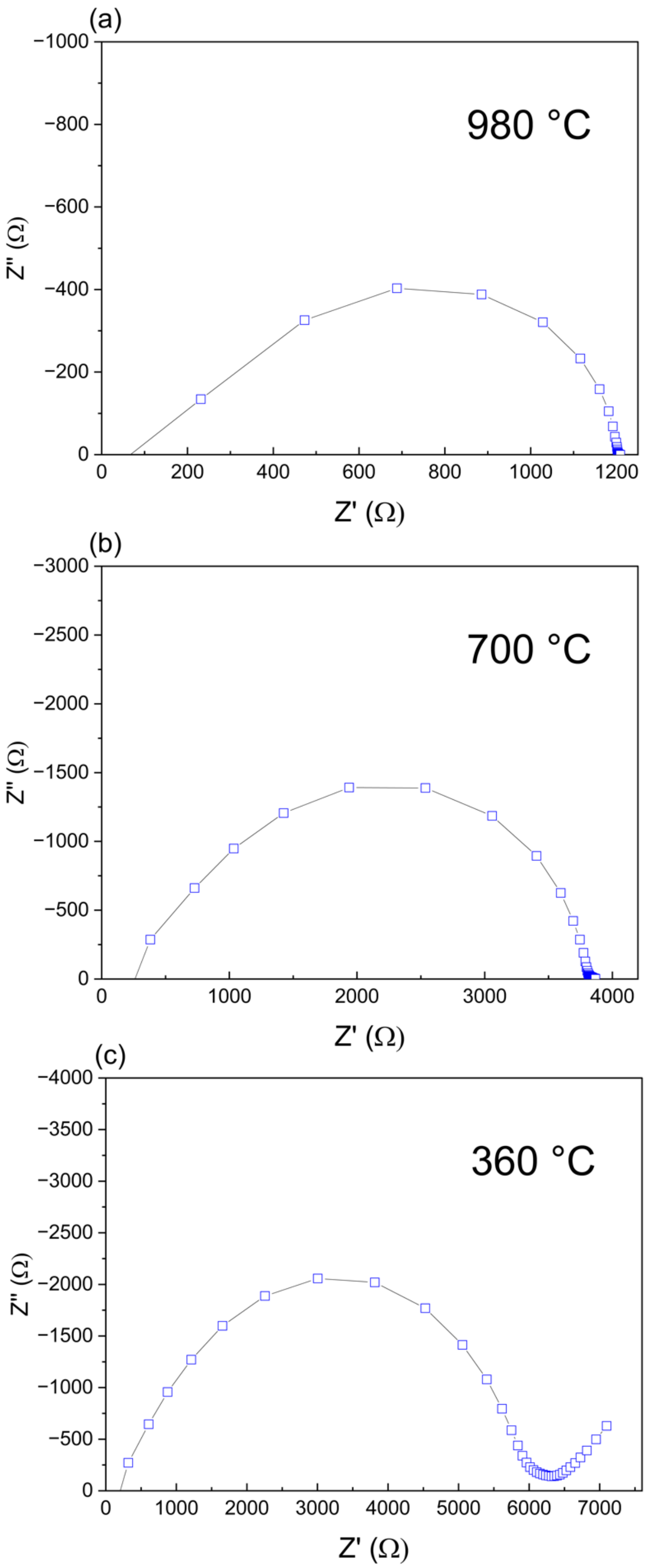

Figure S20: Example impedance spectra of $Ba_5Er_2Al_2SnO_{13}$ as measured in laboratory air at temperatures of 980 °C (a), 700 °C (b) and 360 °C (c)

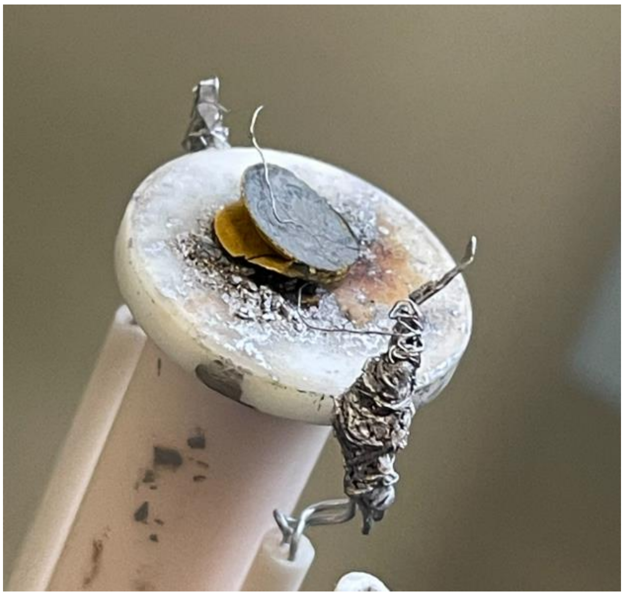

Figure S21: Mounted pellet of $Ba_5Tb_2Al_2SnO_{13}$ after conductivity measurement in wet N_2, showing that the pellet has cracked in half due to significant decomposition.

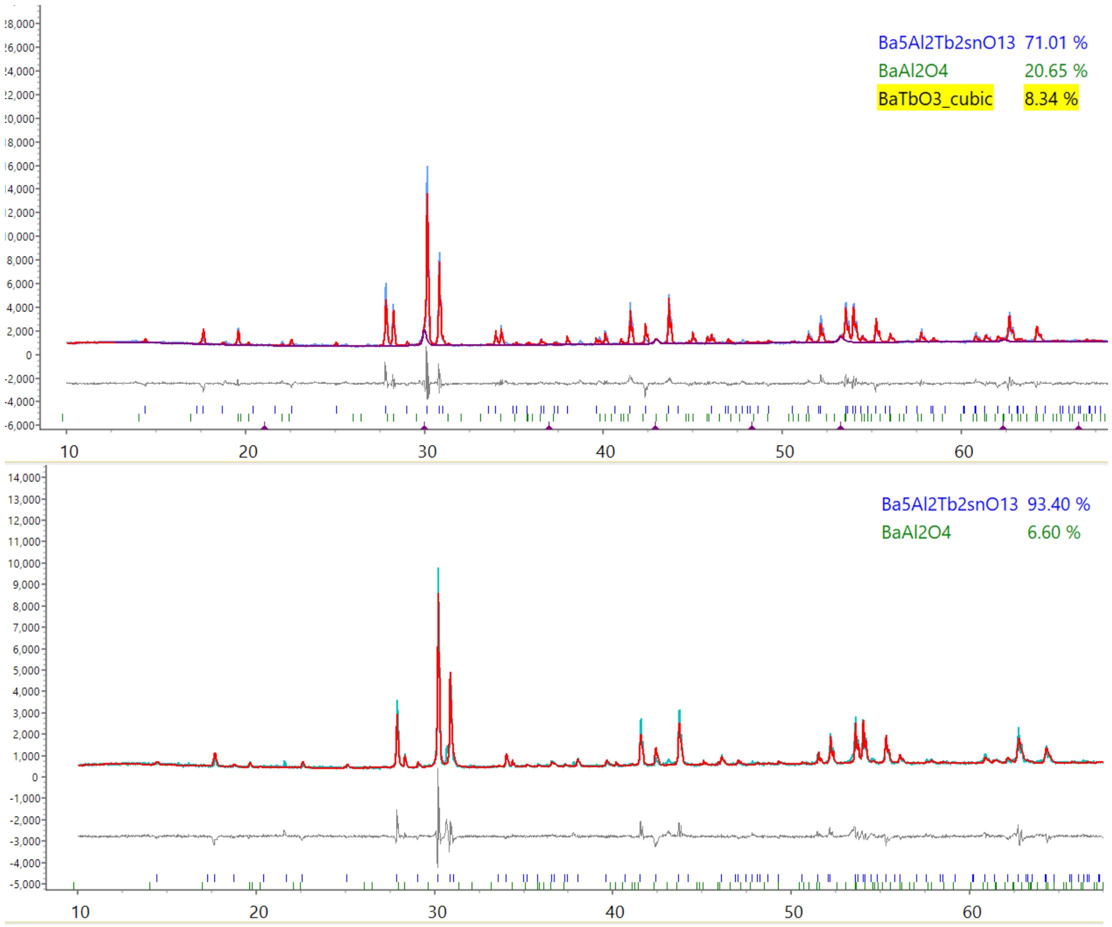

Figure S22: XRPD of a $Ba_5Tb_2Al_2SnO_{13}$ pellet after (top) and before (bottom) conductivity measurement in wet N_2. After exposure in the wet atmosphere the proportion of the $BaAl_2O_4$ phase fraction has substantially increased and $BaTbO_3$ also appears as an additional impurity after the pellet has cracked and most likely undergone partial decomposition.

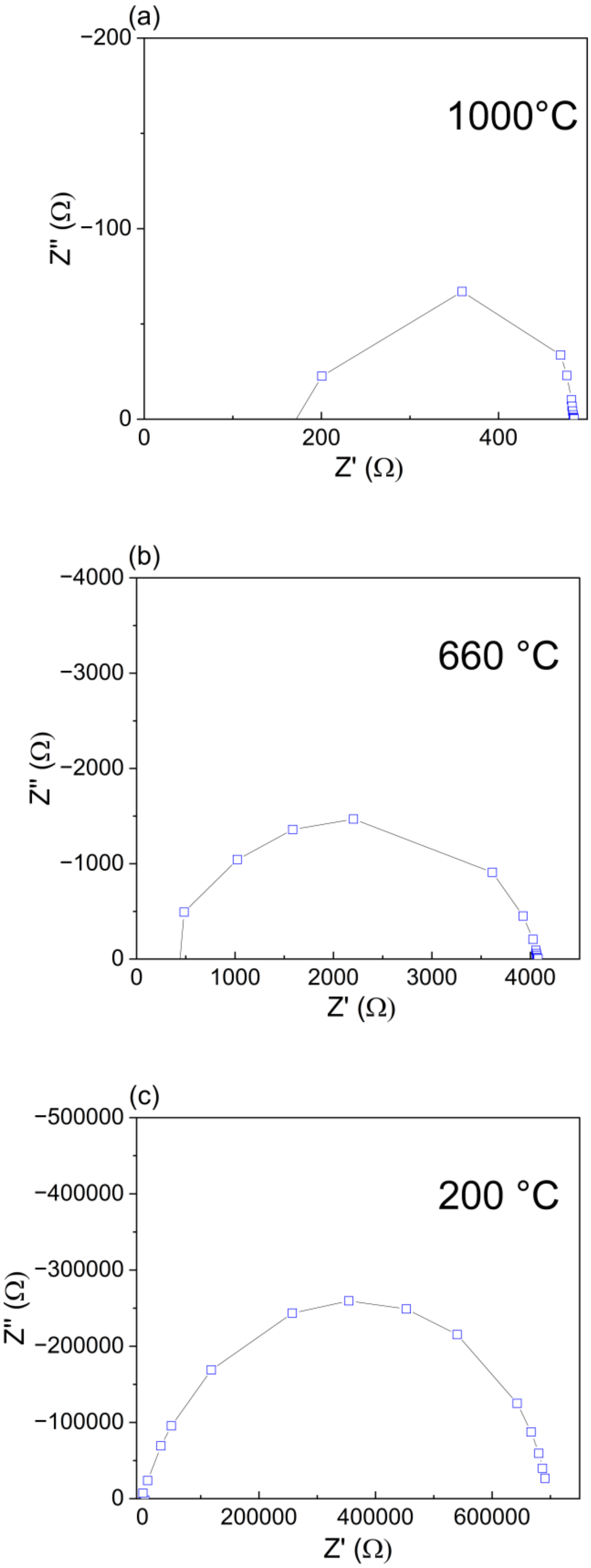

Figure S23: Example impedance spectra of $BaTbAl_2SnO_{13}$ as measured in laboratory air at temperatures of 100 °C (a), 660 °C (b) and 200 °C (c)